PERGAMON

Atmospheric Environment 36 (2002) 2297–2307

ATMOSPHERIC ENVIRONMENT

www.elsevier.com/locate/atmosenv

A modeling study of air pollution modulation through land-use change in the Valley of Mexico ☆

Aron D. Jazcilevich*, Agustín R. García[1], L. Gerardo Ruíz-Suárez

Centro de Ciencias de la Atmósfera, Universidad Nacional Autónoma de México, 04510 D.F., Mexico

Received 12 June 2001; accepted 10 February 2002

Abstract

Using a prognostic air quality model it is shown that by the partial recovery of Lake Texcoco near the Metropolitan Area of Mexico City, a local reduction of about 11% to 15% can be achieved in concentration levels of ozone (O_3), carbon monoxide (CO), sulphur dioxide (SO_2) and chemical compounds with the potential of forming aerosols. This phenomenon takes place because of the land–lake breeze effect and local temperature modulation induced by the location and size of the recovered lake areas. © 2002 Elsevier Science Ltd. All rights reserved.

Keywords: Mexico city; Air pollution modeling; Air quality; Land–lake breeze effect

1. Introduction

In the Metropolitan Area of Mexico City (MAMC) the norm for ozone (O_3) is violated almost 70% of the days of the year (Gobierno del Distrito Federal, 1999). Although this situation will not improve unless vehicular and industrial emissions are drastically reduced, other environmental actions can help to alleviate the situation.

In this paper, using a state of the art air quality model, it is shown that the partial recovery of what once was Lake Texcoco near the MAMC could be a beneficial factor in locally reducing O_3, sulphur dioxide (SO_2), carbon monoxide (CO), and gases that have the potential of forming aerosols that we call here GPAs. They include sulphuric acid (H_2SO_4), nitric acid (HNO_3), unsaturated dicarbonyl, organic nitrate, peroxyacetyl nitrate and higher PANs, TPAN ($CHCO_3NO_2$), formic acid and higher acids, cresol and other hydroxy substituted aromatics.

The proposed recovery area covering an area of $9 \times 15\ km^2$ is located in an arid uninhabited area that is partially flooded during the rainy season. It is the remaining lakebed of Lake Texcoco which was dessicated to prevent floodings. For an historic overview of this event and its consequences in the thermal climate see Jazcilevich et al. (2000). Currently there are plans to partially recover this area as part of a comprehensive hydraulic overhaul in the Valley of Mexico (Jauregui and Jazcilevich, 2000).

2. The air quality model

The air quality model used in this work is the Multiscale Climate Chemistry Model (MCCM) that has been implemented for the central region of Mexico (Garcia et al., 2000). The model includes modules for meteorology, photolysis, biogenic emissions, radiation, and deposition among others. The meteorological module of MCCM is based on the fifth-generation Penn State/NCAR Mesoscale Model called MM5, see Grell et al. (1994). It is widely used by the meteorological community. MM5 is non hydrostatic with terrain following coordinates, has a multi-scale option, is capable of four-dimensional data-assimilation, has an

☆ Partially supported by grant RI-500-5-1 CONACYT-RED.

*Corresponding author.

E-mail addresses: jazcilev@servidor.unam.mx (A.D. Jazcilevich), agustin@atmosfera.unam.mx (A.R. García), ruizs@servidor.unam.mx (L.G. Ruíz-Suárez).

[1] Ph.D. scholarship by CONACYT.

PII: S1352-2310(02)00197-8

interface with actual weather forecast models (GCM and observations), contains explicit cloud schemes and multilevel soil/vegetation parameterization.

An advantage of MCCM is that the meteorological model is directly coupled with a chemistry-transport-model and a photolysis module. The biogenic emissions module is coupled with radiation and RADM2 (Stockwell et al., 1995), chemical mechanism. Also, a deposition module is coupled with higher order closure turbulence parameterization, a WALCEK aqueous phase chemistry extension to RACM can be used, and a third-order Smolarkiewicz scheme is used for pollutant advection. For a detailed description of this see Grell et al. (2000).

The gas phase chemistry used in this study was RADM2 (Stockwell et al., 1995). This mechanism considers for the inorganic part, 14 stable species, 4 reactive intermediaries and 3 abundant-stable species. The organic part considers 26 stable species and 16 peroxy radicals. The photo-chemistry is based on the aggregated molecular approach for reactivity (Middleton et al., 1990). The photolysis module uses a radiative transfer model. This module calculates photolysis frequencies for reaction gas phase chemistry that considers changes in the radiation with height and changes in air composition such as O_3, aerosols and water vapor. The version used here of MCCM does not include a module for aerosol formation and should be considered as a limitation.

The biogenic module calculates organic emissions of isoprene, monoterpenes and other organic and inorganic compounds such as nitrogen soil emissions. This kind of emissions depends on temperature, radiation and type of vegetation. The dry deposition module calculates the elimination of trace compounds from the atmosphere depending on deposition velocity which is calculated using aerodynamic, sub-layer and surface resistance (Wesley, 1989).

The emissions inventory includes mobile, point and area sources. These data is obtained from emission inventories performed by the city government (Gobierno del Distrito Federal, 1995). The compounds considered are nitrogen oxides (NO_x), sulfur dioxide (SO_2), carbon monoxide (CO) and volatile organic compounds (VOC).

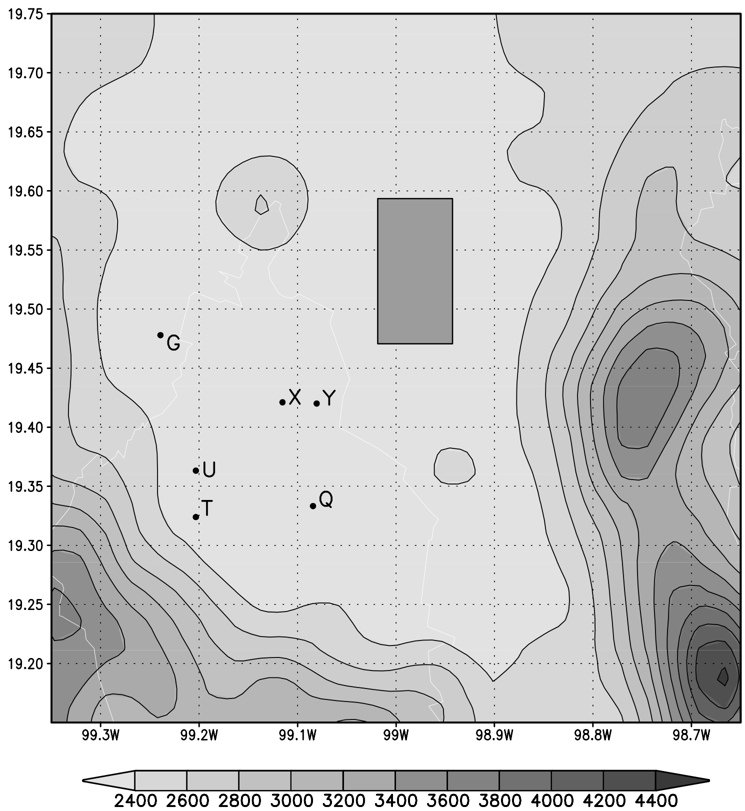

Fig. 1. Topography and virtual lake location denoted by a rectangle. The RAMA stations used for comparisons are Acatlan (G), Estrella (Q), Merced (X), Pedregal (T), Plateros, (U) and Hangares (Y). Heavily populated areas of the MAMC lie to the west and southwest of the virtual lake.

The temporal resolution of the emissions model is 1 h and the spatial resolution is 2 km. The emissions inventory domain includes an area of 32,400 km^2.

The emissions were divided into two classes depending on their source: anthropogenic due to human activities and biogenic mainly due to forests and farmland. Although the first class represents the main contribution to emissions, the emissions from natural sources could represent, in some cases an important source of the emissions of VOCs (Ruiz-Suarez et al., 1999; Lamb et al., 1987).

3. Experiments with the lake

The MCCM model is used to test the local influence on climate and on the concentrations of O_3, GPAs, NO_x, SO_2 and CO concentrations of a virtual lake placed in the northeast of Mexico City, see Fig. 1.

The time period for the computational experiments takes place during the dry winter season, from 25 to 28 February 1997. During winter, high pollution episodes are common due to inversion layers and sun radiance capable of driving the photochemistry to high O_3 concentrations.

Three one-way nested domains are used as shown in Fig. 2 for the experiments.

Two computational experiments are performed: The first consists of the model running with present day land use, while in the second a virtual lake is formed by placing a water body using the land use facility of MCCM, as shown in Fig. 1. In both cases same initial and boundary conditions for the outmost domain are used.

The purpose of the first experiment is to show that MCCM is capturing correctly the meteorology and reproducing the air pollution phenomenon. Once this is

Table 1
Statistical analysis for surface temperature

Station	Acatlan	Estrella	Merced	Pedregal	Plateros	Hangares
CC	0.95	0.95	0.95	0.95	0.96	0.95
RMSE	2.02	1.71	1.65	2.99	1.48	1.50
$RMSE_s$	1.57	1.21	0.88	2.79	1.37	0.78
$RMSE_u$	1.28	1.21	1.40	1.07	1.08	1.28
d	0.95	0.96	0.96	0.90	0.96	0.95
$\frac{RMSE_s}{RMSE}$	0.78	0.71	0.53	0.93	0.92	0.52
$\frac{RMSE_u}{RMSE}$	0.63	0.71	0.85	0.36	0.73	0.85

Note: CC correlation coefficient, RMSE root mean square error, $RMSE_s$ root mean square error systematic, $RMSE_u$ root mean square error unsystematic, d index of agreement.

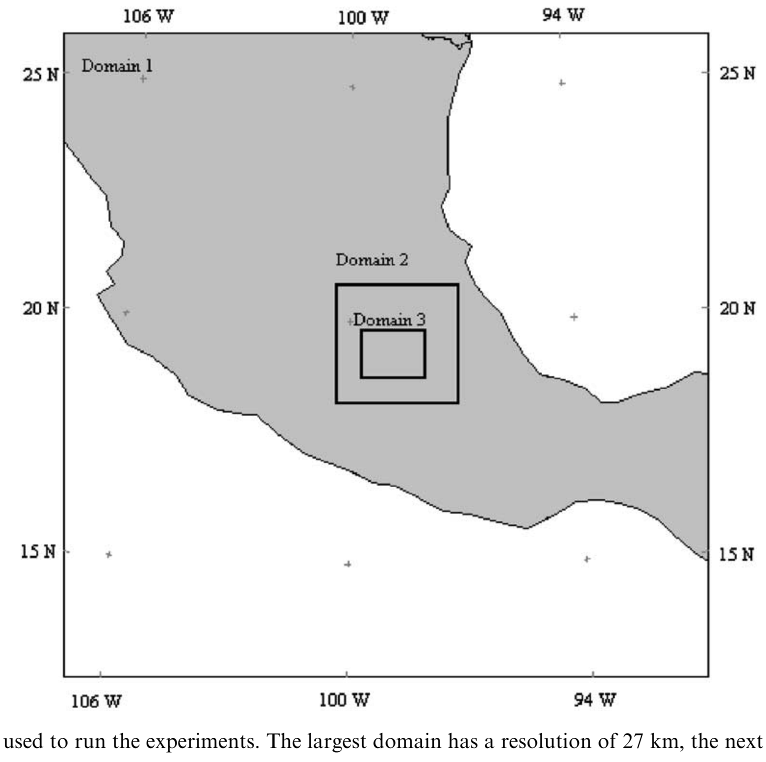

Fig. 2. Nested domains used to run the experiments. The largest domain has a resolution of 27 km, the next domain of 9 km, and the innermost 3 km.

Table 2
Statistical analysis for surface wind intensity

Station	Acatlan	Estrella	Merced	Pedregal	Plateros	Hangares
CC	0.40	0.60	0.48	0.36	0.27	0.64
RMSE	1.28	1.08	0.89	0.77	0.80	1.42
$RMSE_s$	0.52	0.63	0.36	0.50	0.49	1.18
$RMSE_u$	1.17	0.88	0.81	0.58	0.64	0.79
d	0.65	0.59	0.69	0.52	0.55	0.71
$\frac{RMSE_s}{RMSE}$	0.41	0.58	0.40	0.65	0.61	0.69
$\frac{RMSE_u}{RMSE}$	0.91	0.81	0.91	0.75	0.80	0.46

Note: CC correlation coefficient, RMSE root mean square error, $RMSE_s$ root mean square error systematic, $RMSE_u$ root mean square error unsystematic, d index of agreement.

Table 3
Statistical analysis for surface O_3

Station	Acatlan	Estrella	Merced	Pedregal	Plateros	Hangares
CC	0.74	0.65	0.79	0.69	0.71	0.68
RMSE	0.04	0.06	0.04	0.06	0.05	0.05
$RMSE_s$	0.03	0.05	0.01	0.05	0.03	0.03
$RMSE_u$	0.03	0.03	0.03	0.04	0.04	0.04
d	0.76	0.74	0.88	0.42	0.79	0.78
$\frac{RMSE_s}{RMSE}$	0.75	0.83	0.25	0.83	0.60	0.60
$\frac{RMSE_u}{RMSE}$	0.75	0.50	0.75	0.67	0.80	0.80

Note: CC correlation coefficient, RMSE root mean square error, $RMSE_s$ root mean square error systematic, $RMSE_u$ root mean square error unsystematic, d index of agreement.

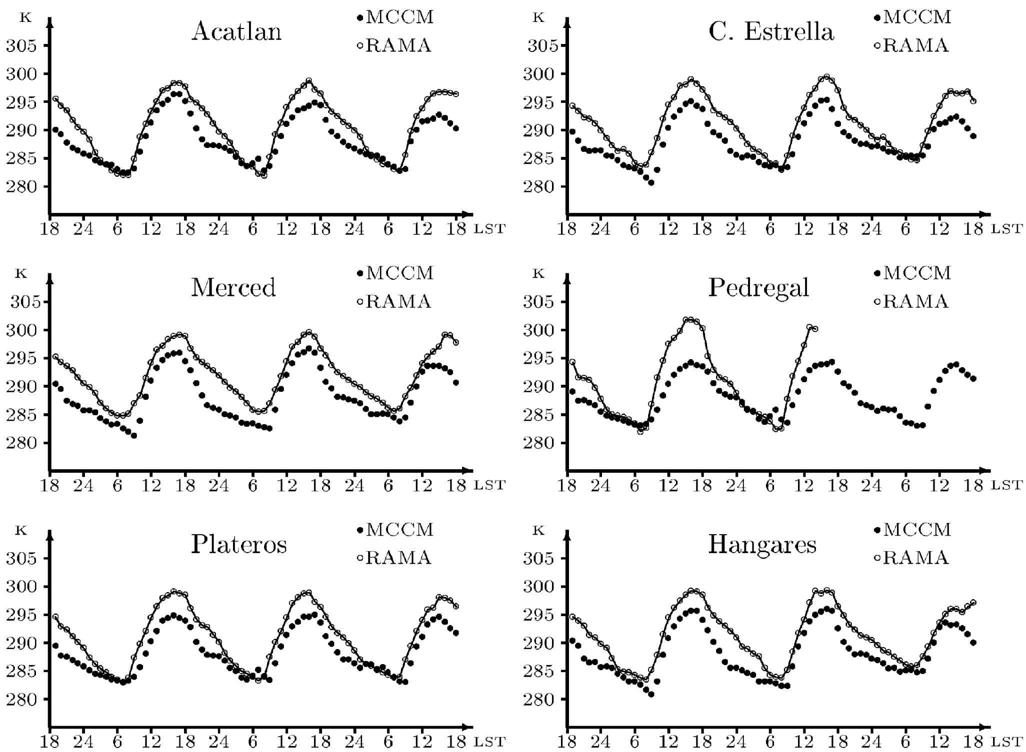

Fig. 3. Temperature profiles using MCCM and measurements at selected RAMA stations.

established, the results of the second experiment with the virtual lake is well founded.

3.1. First experiment: present day land use

Tables 1 and 2 show a statistical error analysis for modeled temperature and wind intensity, respectively, using data provided by a selection of typical stations of the automatic monitoring network named RAMA, that overall operates 20 stations in the valley.

It can be seen that the index of agreement d (see Willmott, 1981), for temperatures is above 0.90 and reaches above 0.95 in stations Hangares and Merced which are the nearest to the lake area. The wind intensity d is above 0.50 and reaches above 0.68 for stations Hangares and Merced. Overall d achieves relatively high values specially near the lake area. Similar satisfactory results were obtained for the other statistical parameters. It should be noted that all these statistical results are significatively better than other studies carried in the area, Instituto Mexicano del Petroleo, 1994 IMP-Los Alamos (1994).

Table 3 shows a statistical analysis for O_3 for same RAMA stations as above. Except for Pedregal, high values for d are achieved, specially for stations Hangares and Merced.

Fig. 3 shows time series for modeled and measured surface temperatures for selected RAMA stations. Fig. 4 shows time series comparing measured and modeled O_3 concentrations for the same selected RAMA stations. These figures, together with the statistical analysis show that the model is reproducing satisfactorily the meteorological and pollution phenomena in the valley.

3.2. Second experiment—virtual lake

A virtual lake of dimensions $9 \times 15\ km^2$ is placed in the northeast of Mexico City, as seen in Fig. 1. The lake temperature was chosen at 15°C, since an existing small lake on the area has this average surface temperature for February (Martinez, 1999). The southwest corner of our virtual lake is about 12 km from the Historic District, the largest gas emissions zone of mobile and area sources in the city.

3.2.1. Meteorological effects of the lake

A consequence of the placement of the virtual lake is that a land–water breeze effect is created because the temperature contrast between water and land produces a pressure gradient. For example, in Fig. 5 it can be seen how the wind field shows a radial pattern out of the lake for day time hours. A downdraft with peak vertical

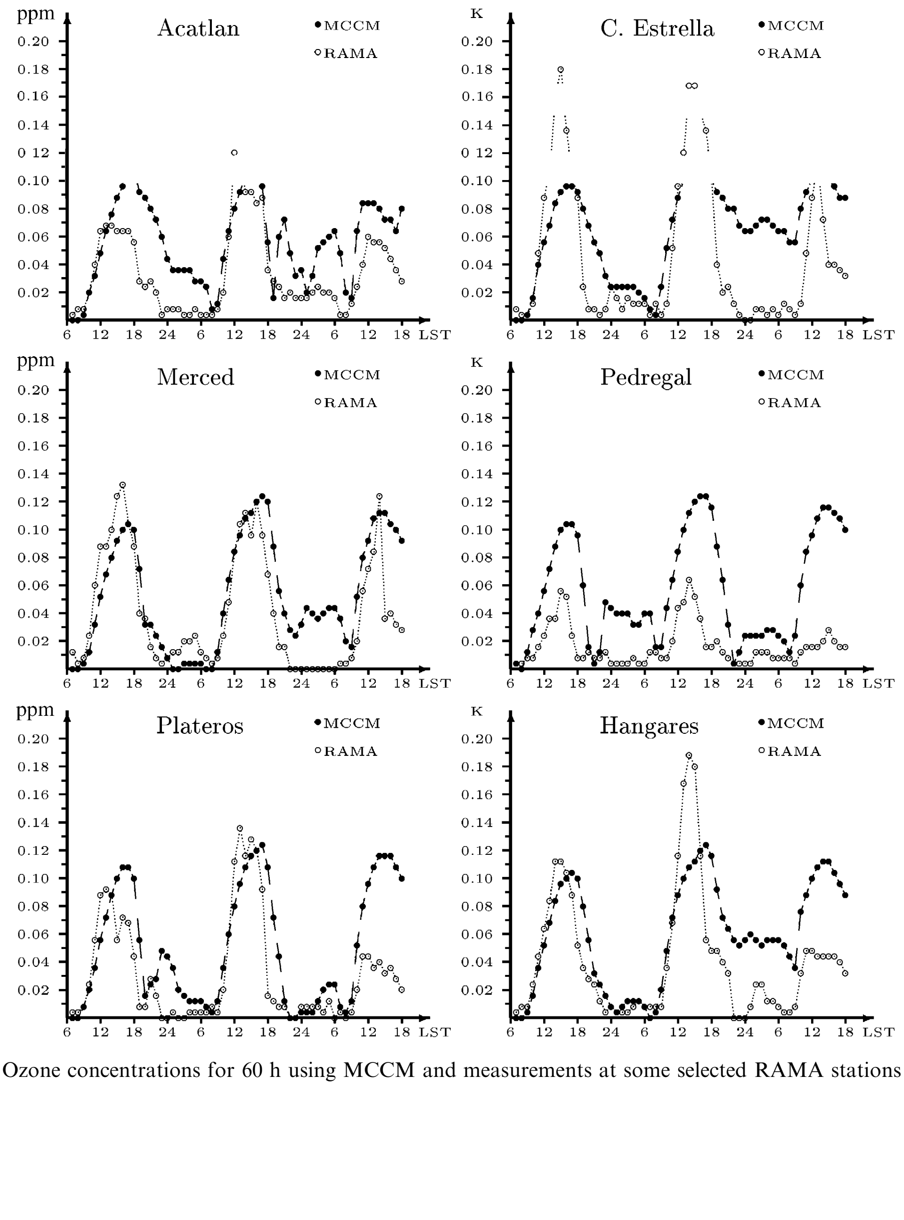

Fig. 4. Ozone concentrations for 60 h using MCCM and measurements at some selected RAMA stations in ppm.

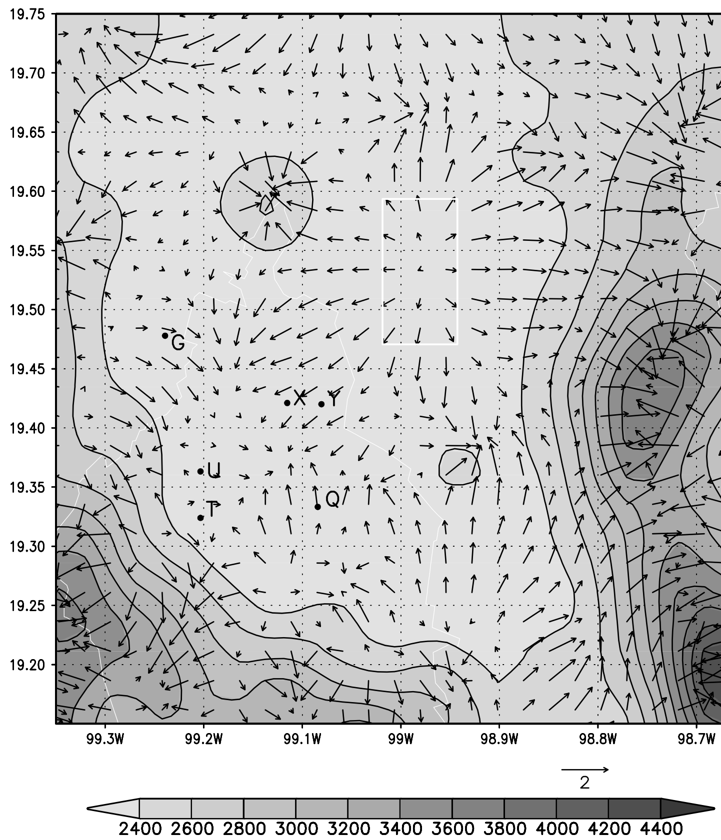

Fig. 5. Modeled average surface wind field from 10:00 to 15:00 LST for the second modeling day with the lake present. Note the land–lake effect producing a radial pattern going out form the lake.

velocities on the center of the lake of about 0.041 m s^{-1} is present. During the night and early morning the radial pattern is reversed although much weaker, as shown in Fig. 6. An updraft with vertical velocities of up to 0.012 m s^{-1} is present on the center of the lake.

We discuss the effect of the lake for day time hours since it is then when the lake presence has its major effect and most of the population is exposed to pollution.

Fig. 7 shows the difference between the average surface temperatures with and without the lake for the second modeling day from 10:00 to 15:00 LST. This figure shows the area where the temperature was influenced by the lake for this day. Also shown is how the lake presence modulates temperature close to it, i.e., because of the lake, peak temperatures during the day are lower and low temperatures during the night are higher.

Fig. 8 shows a difference in average surface O_3 concentrations with and without the lake for the second modeling day from 10:00 to 15:00 LST. Because of the presence of the lake, an area of reduction in O_3 concentrations is formed above a heavily populated area of the MAMC. To study the behavior of O_3 concentrations in the area where maximum average concentrations reduction were obtained a probe P2 is placed inside. A time series comparing surface O_3 concentrations with and without the lake at the probe site P2 is shown in this figure. O_3 peak concentrations have been reduced by about 12%.

Fig. 9 shows a difference in average surface concentrations for GPAs with and without the lake for the second modeling day from 10:00 to 15:00 LST. Once more an area of reduction in concentrations can be seen over a heavily populated area. Pollution levels over the lake area for GPAs are higher because an increase in humidity and lower temperatures reduce the height of the mixing layer. Probe site P3 is placed inside the area with maximum average concentrations reductions that was formed over the heavily populated area. The corresponding time series shows that for the second day peak concentrations were reduced by about 11%.

The behavior for SO_2 is shown in Fig. 10. The maximum reduction in SO_2 concentrations at the corresponding probe site P4 was of about 15%.

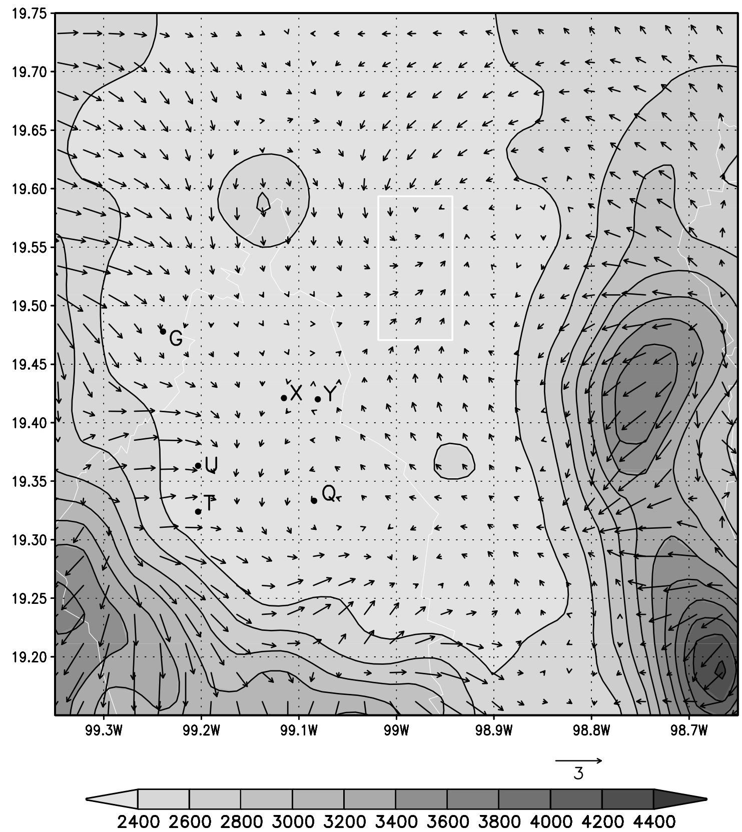

Fig. 6. Modeled average surface wind field from 3:00 to 8:00 LST for the second modeling day with the lake present. Note the land–lake effect producing a radial pattern going into the lake.

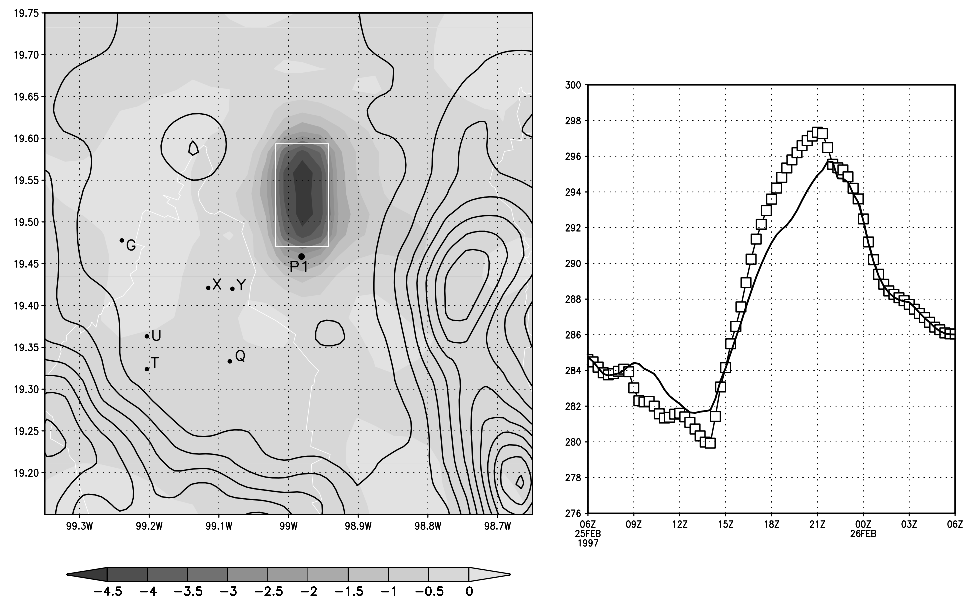

(a) (b)

Fig. 7. Modeled average surface temperature field from 10:00 to 15:00 LST for the second modeling day with the lake present. At right surface temperatures with (·) and without lake (□) at probe site P1 for second modeling day from 0:00 to 23:00 LST.

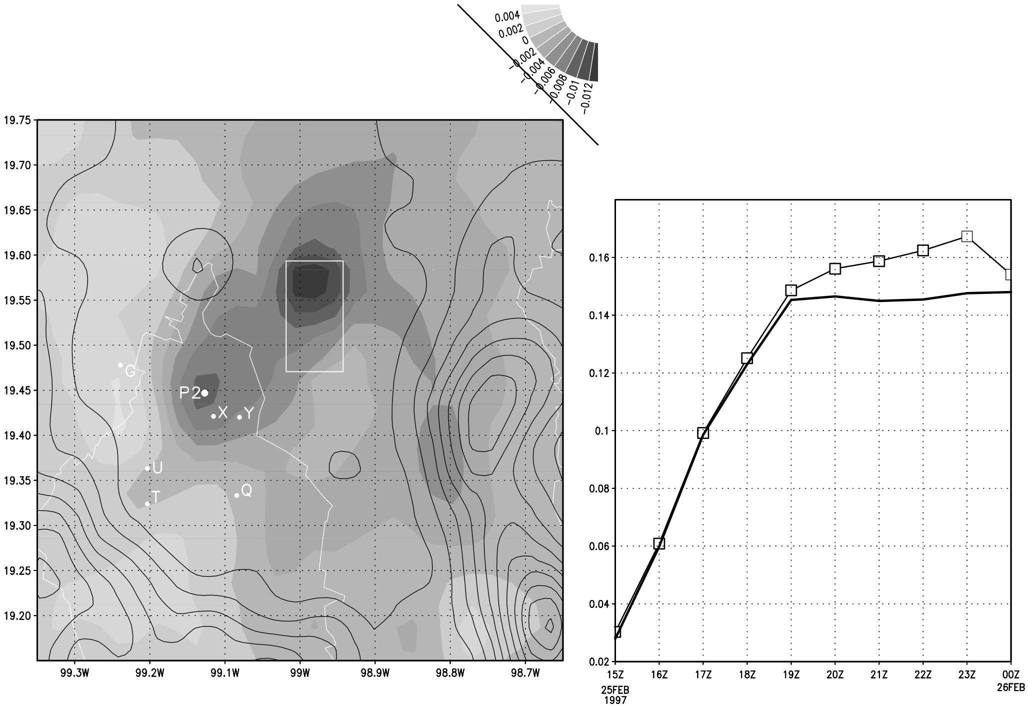

(a) (b)

Fig. 8. Modeled average O_3 concentrations difference from 10:00 to 15:00 LST. At right O_3 concentrations with (·) and without lake (□) at probe P2 for second modeling day from 9:00 to 18:00 LST. O_3 concentrations have been modulated. A peak reduction due to the lake of about 12% has been achieved.

Fig. 11 shows the results for CO. Because of the presence of the lake, a reduction area in CO concentrations over populated areas is present. At the location of probe site P5 concentrations decreased by about 12%.

For NO_x the difference between the lake and no-lake cases are negligible, and concentrations differences are less than 3% as shown in Fig. 12 for probesite P6.

Because of the presence of the lake, nighttime concentration peaks of all pollutants considered here also decrease over the populated area in the southwest of the lake, except for CO whose peak increased by about 12% to about 6.2 ppm, well within local normative values (13 ppm for 8 h of exposure).

4. Conclusion

Two effects take place because of the presence of the lake: the land–lake breeze and temperature modulation. The lake–land breeze effect tend to attract pollutants during the night and early morning hours. The slight updraft and vertical diffusion send the pollutants upward. During day hours these pollutants come down and tend to disperse when they are advected radially as shown in Fig. 5.

Although the temperature changes are not severe, they have an influence on O_3 concentrations because second order molecular reactions decrease its reactivity with decrease in temperature while third order molecular reactions (termination chain reactions) increase its reactivity with the temperature decrement. Therefore lower temperatures tend to delay and reduce O_3 peaks, and vice versa when temperatures increase, see Mulcahy (1973).

The results obtained for the modeling period show that for the second modeling day a reduction in peak O_3 of about 12% was obtained in the southwest area of the lake where probe P2 is located. Peak reduction of about 11% for GPAs at probe site P3 also in the southwest of the lake was obtained. SO_2 concentrations were also reduced. We tried to enhance the reductions of SO_2 by placing grass in the southern and eastern shores of the virtual lake. This situation increased the area of reduction for this and other pollutants, but did not affect much the peaks. CO concentrations also decreased in the southwest of the lake. NO_x concentrations did not show much variation for the two experiments.

The influence of the lake has been beneficial since O_3, SO_2, CO and GPAs concentrations have been reduced significantly in areas inside the MAMC. Higher peak reductions (20% for O_3) with a more pronounced

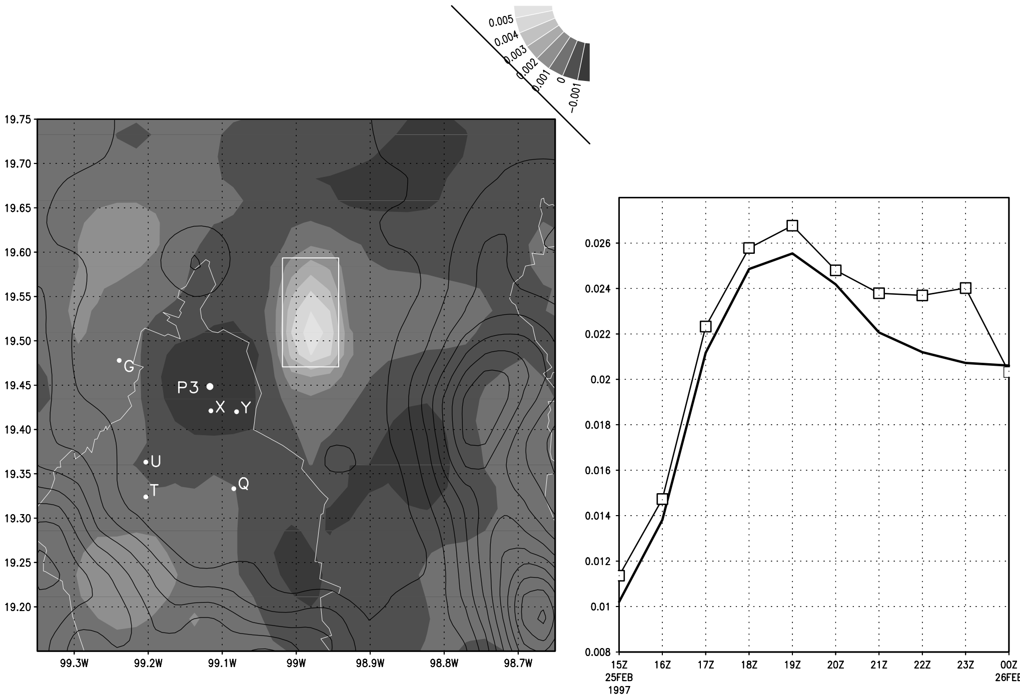

(a) (b)

Fig. 9. Modeled average GPA concentrations difference from 10:00 to 15:00 LST. At right GPAs concentrations with (·) and without lake (□) at probe P3 for second modeling day from 9:00 to 18:00 LST. GPAs concentrations have been modulated. A peak reduction due to the lake of about 11% has been achieved.

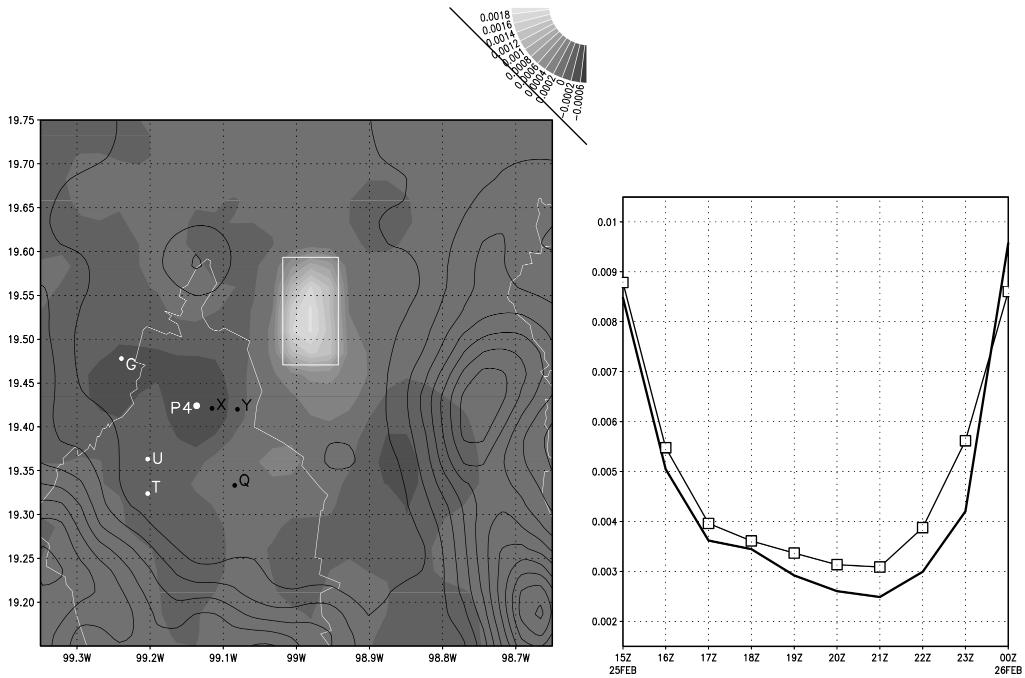

(a) (b)

Fig. 10. Modeled average SO_2 concentrations difference from 10:00 to 15:00 LST. At right SO_2 concentrations with (·) and without lake (□) at probe P4 for second modeling day from 9:00 to 18:00 LST. SO_2 concentrations have been reduced. A maximum reduction in concentrations due to the lake of about 15% has been achieved.

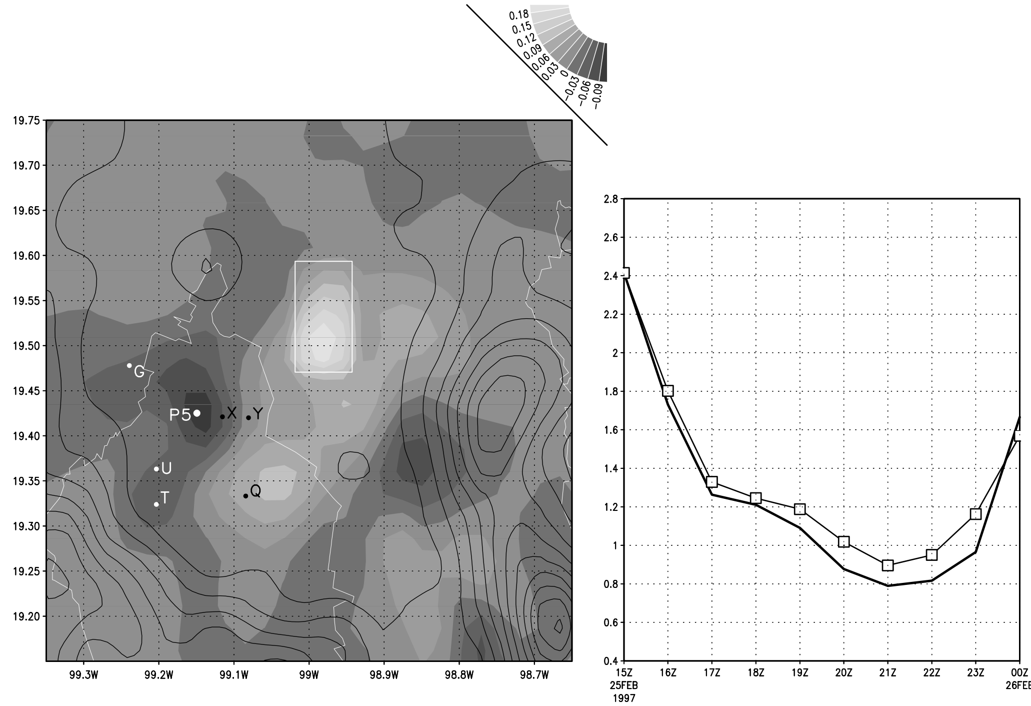

(a) (b)

Fig. 11. Modeled average CO concentrations difference from 10:00 to 15:00 LST. At right CO concentrations with (·) and without lake (□) at probe P5 for second modeling day from 9:00 to 18:00 LST. Maximum reduction of about 12% has been achieved.

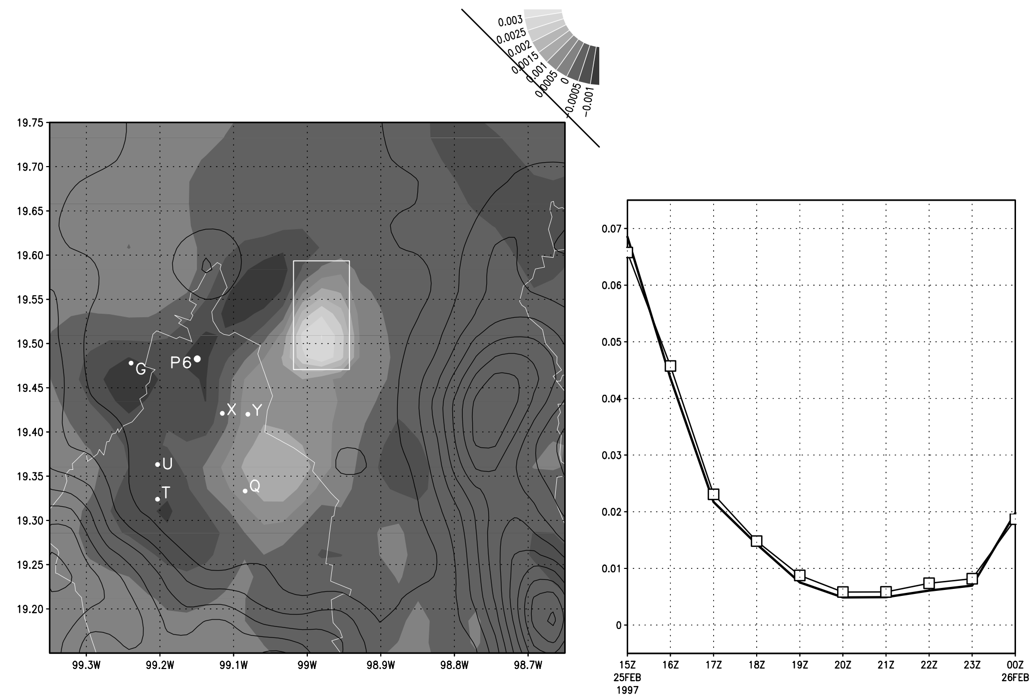

(a) (b)

Fig. 12. Modeled average NO_x concentrations difference from 10:00 to 15:00 LST. At right with (·) and without lake (□) at probe P6 for second modeling day from 9:00 to 18:00 LST. NO_x concentrations are almost identical for both experiments.

modulation were obtained in other experiments not shown here when the reduction area fell in the northeast of the lake, outside the MAMC where much lower emissions are found.

Regions where significantly surface O_3, SO_2, CO and GPA concentrations modulation takes place are about 10–15 km away from the lake. These areas are variable in size and location depending on wind direction. The effect is local but in our case affects important populated areas.

In an experiment similar to ours where soil moisture values were increased in the Los Angeles area (Jacobson, 1999), no beneficial effect on air quality was found. An important difference is that in our case, the proposed lake location and size induces a surface air flow resulting in a change in the air quality.

Because of the modulation effect on concentrations of important pollutants such as O_3, SO_2, CO and GPAs, the recovery of Lake Texcoco can have a positive impact on a localized but numerous population. This result shows the beneficial effect of water bodies when they are judiciously placed near a metropolitan area. This factor can be important for city planners.

Acknowledgements

We acknowledge Ernesto Jauregui who suggested the idea in one of our talks.

References

Garcia, R.A., Schoenemyer, T., Jazcilevich, D.A., Ruiz-Suarez, G., Fuentes-Gea, V., 2000. Implementation of the Multiscale Climate Chemistry Model (MCCM) for Central Mexico. Air Pollution VII. ISBN 1-85312-822-8. In: Longhurst, J.W.S., Brebbia, C.A., Power, H. (Eds.), WIT Press, pp. 71–78.

Gobierno del Distrito Federal, 1995. Inventario de fuentes de area precursores de ozono y monoxido de carbono para la zona metropolitana de la ciudad de México 1995, DDF-Subdireccion de inventario de emisiones.

Gobierno del Distrito Federal, 1999. Compendio Estadistico de la Calidad del Aire, 1986–1999, Secretaria del Medio Ambiente, pp. 25.

Grell, G.A., Dudhia, J., Stauffer, D.R., 1994. A description of the fifth-generation Penn State/NCAR Mesoescale Model (MM5). NCAR Technical Note TN-398 + SRT.

Grell, G.A., Emei, S., Stockwell, W.R., Schoenemeyer, T., Forkel, R., Michalakes, J., Knoche, R., Seild, W., 2000. Application of a multiscale, coupled MM5/Chemistry model to the complex terrain of the VOLTAP valley campaign. Atmospheric Environment 34, 1435–1453.

Instituto Mexicano del Petroleo, 1994. Mexico City Air Quality Research Institute, Vol. III.

Jacobson, M.Z., 1999. Effects of soil moisture on temperatures, winds and pollutant concentrations in Los Angeles. Journal of Applied Meteorology 38, 607–616.

Jauregui, E., Jazcilevich, D.A., 2000. Cambios Climatologicos Potenciales con la Instalacion de Nuevos Lagos en la Cuenca del Valle de Mexico. Reporte Preliminar, Rescate del Lago de Texcoco, Proyecto Ecologico.

Jazcilevich, D.A., Fuentes, V., Jauregui, E., Luna, E., 2000. Simulated urban climate response to historical land use modification in the Basin of Mexico. Climatic Change 44, 515–536.

Lamb, B., Geuther, A., Gay, D., Westberg, H., 1987. A national inventory of biogenic hydrocarbons emissions. Atmospheric Environment 21, 1695–1705.

Martinez, I., 1999. Seguridad Lago Nabor Carrillo, Data-Logbook.

Middleton, P., Stockwell, W.R., Carter, W.P.L., 1990. Aggregation and analysis of volatile organic compound emissions for regional modeling. Atmospheric Environment 24A, 1107–1133.

Mulcahy, M.F.R., 1973. Gas Kinetics, Thomas Nelson and Sons, Ltd., pp. 19–20.

Ruiz-Suarez, L.G., Longoria, R., Hernandez, F., Segura, E.H., Trujillo, A., Conde, C., 1999. Emisiones biogenicas de hidrocarburos no-metano y de oxido nitrico en la cuenca del valle de Mexico. Atmosfera 12, 89–100.

Stockwell, W.R., Middleton, R.P., Chang, J.S., Tang, X., 1995. The second generation regional acid deposition model chemical mechanism for regional air quality modeling. Journal of Geophysical Research 95, 16343–16367.

Wesley, M.L., 1989. Parametrization of surface resistance to gaseous dry deposition in regional numerical models. Atmospheric Environment 16, 1293–1304.

Willmott, C.J., 1981. On the validation of models. Physical Geography 2, 184–194.